MOLECULAR PHYSICS, 2002, VOL. 100, NO. 15, 2397–2415

A computer simulation study of racemic mixtures

J. LARGO[1,2], C. VEGA[1]*, L. G. MACDOWELL[1] and J. R. SOLANA[2]

[1] Departamento de Química Física, Facultad de Ciencias Químicas, Universidad Complutense, 28040 Madrid, Spain

[2] Departamento de Física Aplicada, Universidad de Cantabria, 39005 Santander, Spain

(*Received 5 July 2001; accepted 2 November 2001*)

A simple model for a chiral molecule is proposed. The model consists of a central atom bonded to four different atoms in tetrahedral coordination. Two different potentials were used to describe the pair potentials between atoms: the hard sphere potential and the Lennard-Jones potential. For both the hard sphere and the Lennard-Jones chiral models, computer simulations have been performed for the pure enantiomers and also for the racemic mixture. The racemic mixture consisted of an equimolar mixture of the two optically active enantiomers. It is found that the equations of state are the same, within statistical uncertainty, for the pure enantiomer fluid and for the racemic mixture. Only at high pressures does the racemic mixture seem to have a higher density, for a given pressure, than the pure enantiomer. Concering the structure, no difference is found in the site–site correlation functions between like and unlike molecules in the racemic mixture either at low or at high densities. However, small differences are found for the site–site correlations of the pure enantiomer and those of the racemic mixtures. In the Lennard-Jones model, similar conclusions are drawn. The extension of Wertheim's first-order perturbation theory, denoted bonded hard sphere theory (ARCHER, A. L., and JACKSON, G., 1991, *Molec. Phys.*, **73,** 881; AMOS, M. D., and JACKSON, G., 1992, *J. chem. Phys.*, **96,** 4604), successfully reproduces the simulation results for the hard chiral model. Virial coefficients of the hard chiral model up to the fourth have also been evaluated. Again, no differences are found between virial coefficients of the pure fluid and of the racemic mixture. All the results of this work illustrate the quasi-ideal behaviour of racemic mixtures in the fluid phase.

1. Introduction

The study of molecular fluids and their mixtures has been one of the central topics in statistical thermodynamics over the last 30 years. The influential book of Gray and Gubbins [1] has been an invaluable reference to anyone interested in applying the methods of statistical thermodynamics to molecular systems. Their work on spherical and linear molecules, with or without a multipole, has proved to be an obligatory reference to any one interested in the behaviour of bulk [2–4] molecular fluids. In the late 1980s, Gubbins along with Chapman and Jackson [5, 6] illustrated the enormous potential for practical applications hidden in Wertheim's theory of association, and how this theory could be applied successfully to chains [7–9].

This paper is devoted to a special type of molecular fluid that has received little attention: the fluid behaviour of simple chiral models. Molecules lacking an inversion-rotation axis (i.e. S_i axis) exhibit optical activity [10]. Molecules lacking an S_i axis cannot be superposed on their specular image. For common organic molecules the absence of an S_i is associated with the presence of a chiral carbon centre (i.e. a C atom bonded to four different substituents) [11]. When only one chiral carbon centre exists then there are two different optical isomers (also known as enantiomers). These two different enantiomers are usually denoted as R and S [11] (although when dealing with amino acids the notation L and D tends to be used [12]). The two enantiomers exhibit identical physical properties (critical point, viscosity), the only difference being the direction of the rotation of the plane of polarized light.

A racemic mixture consists of an equimolar mixture of the R and S isomers, which results in the lack of optical activity. Quite often (but not always) chemical synthesis leads to the formation of a racemic mixture. An interesting question is the determination of the mixing (excess) properties of mixtures of chiral molecules. If we mix the pure R enantiomer, with the pure S enantiomer then one may measure the excess volume and the excess enthalpy. The number of experimental

* Author for correspondence. e-mail: cvega@eucmos.sim.ucm.es

Molecular Physics ISSN 0026–8976 print/ISSN 1362–3028 online
http://www.tandf.co.uk/journals
DOI: 10.1080/00268970110109871

studies on the excess properties of chiral molecules is limited [13–17]. Certainly these kinds of study are quite difficult since the excess properties of enantiomeric mixtures are quite small [18, 19]. However, there are several studies where these excess properties have been measured experimentally. An open question is the presence of L amino acids in all biological samples (and the absence of D amino acids). It is not clear why all forms of life on earth are using L amino acids instead of the D form [12]. The behaviour of racemic mixtures in the solid phase is also quite interesting [18, 19], since they show rich behaviour: namely, they form solid solutions, racemic compounds (a solid compound of stoichiometry 1:1 is formed in the solid phase), and conglomerates (i.e. separation of R and S crystals by the formation of a eutectic). The classic paper of Pasteur [20] illustrates the formation of conglomerates.

Theoretically, racemic mixtures have received very little attention. Kenney and Deiters [21] studied racemic mixtures from a thermodynamic and molecular point of view, and Vatamanu and Cann [22] performed a theoretical study via an integral equation of the structural properties of racemic mixtures. Vlot *et al.* [23] performed computer simulations of a racemic mixture (although the model used is somewhat questionable, since they used the Lennard-Jones (LJ) potential for the R and S molecules and described the R–S interaction by a different LJ interaction). Other aspects of chiral compounds have been reviewed [24]. These recent papers prompted us to study simple models of chiral compounds.

It is well known that repulsive forces dominate the structure of fluids at high densities [25, 26]. Moreover there are a number of theoretical methods for describing mixtures of hard bodies [27]. Therefore the study, via computer simulation, of a mixture of hard bodies with chiral properties is an interesting problem. In this paper we present *NpT* Monte Carlo simulations of a simple model (methane-like) of a chiral molecule. One of the simplest conceivable models of a chiral molecule is a molecule with a central atom and four different atoms in tetrahedral coordination (although four different atoms would be sufficient for chirality to exist [22]). This model mimics the geometry of a derivative of methane. The model presents two different optical isomers, namely the R and the S. Simulations were performed for one of the pure enantiomers and for the racemic mixture, with the aim of determining whether there are differences in the equations of state and structural properties between the two. In order to analyse the behaviour at low densities, the values of the second, third, and fourth virial coefficients of the pure enantiomer and of the racemic mixture were calculated and are reported here. The effect of introducing attractive forces in the model is also analysed.

2. Model and computational details

2.1. *A primitive model of a chiral hard molecule*

It is well known that derivates of methane with four different substituents atoms are chiral (e.g. CHFClBr). By chiral we mean that the molecule cannot be superposed with its mirror image. Inspired by this fact we shall propose a simple model which we shall denote the hard primitive model (HPM) of a hard chiral molecule. The model consists of a central hard sphere, with a diameter of 1, and four hard spheres, all of them tangent to the former, with diameters given by 0.9, 0.8, 0.7, 0.6, placed in a tetrahedral coordination (with a bonding angle of 109.5° between the central atom and any pair of smaller atoms). The model defined in this way is chiral. The two different optical isomers are denoted as R and S. We shall follow the chemical criterion for the labelling of the R and S enantiomers, according to which the four atoms surrounding the central atom are labelled from the heaviest (1) to the lightest (4). We assume here that the molecular mass of each atom is proportional to its diameter (figure 1 (*a*)). The central atom is located in the plane of the paper and the lightest one is located perpendicular to the plane of the paper moving away from the viewer. If the rotation from atom 1 to 2, and from 2 to 3 is clockwise, the

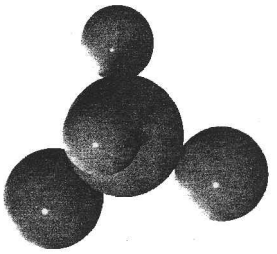

(*a*)

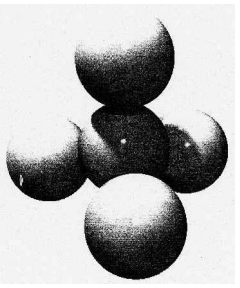

(*b*)

Figure 1. (*a*) Hard primitive model (HPM) of chiral molecule used in this work. (*b*) Tetrahedral model of Sear *et al.* [54].

Table 1. Coordinates of the atoms in enantiomer S of the primitive model. The diameter of the central atom is taken as the unit of length. σ_{ii} denotes the diameter of atom i. l_{1i} denotes the bond length between the central atom (atom 1) and atom i.

Atom	σ_{ii}	x	y	z	l_{1i}
1	1.0	0.0	0.0	0.0	0.0
2	0.9	0.548 482 76	0.548 842 76	0.548 482 76	0.95
3	0.8	−0.519 615 24	−0.519 615 24	0.519 615 24	0.90
4	0.7	−0.490 747 73	0.490 747 73	−0.490 747 73	0.85
5	0.6	0.461 880 22	−0.461 880 22	−0.461 880 22	0.80

Table 2. Coordinates of the atoms in enantiomer R of the primitive model. The diameter of the central atom is taken as the unit of length. σ_{ii} denotes the diameter of atom i. l_{1i} denotes the bond length between the central atom (atom 1) and atom i.

Atom	σ_{ii}	x	y	z	l_{1i}
1	1.0	0.0	0.0	0.0	0.0
2	0.9	0.548 482 76	0.548 842 76	0.548 482 76	0.95
3	0.8	−0.519 615 24	−0.519 615 24	0.519 615 24	0.90
4	0.7	0.490 747 73	−0.490 747 73	−0.490 747 73	0.85
5	0.6	−0.461 880 22	0.461 880 22	−0.461 880 22	0.80

enantiomer is denoted as R, and if it is counterclockwise then the enantiomer is denoted as S [11]. The coordinates of the centre of the five hard spheres forming the S and R enantiomers are presented in tables 1 and 2, respectively. The atoms are labelled from 1 to 5, starting with the central atom (atom 1), atom 2 having diameter 0.9, atom 3 having diameter 0.8, atom 4 having diameter 0.7, and atom 5 having diameter 0.6. The model is rigid in the sense that bond lengths and angles are fixed. All intermolecular interactions between pairs of atoms are hard sphere interactions.

Because the thermodynamic properties of a pure fluid with molecules of type R are identical to those of a pure fluid with molecules of type S we shall study the properties of only the pure R fluid, in addition to the racemic mixture. By contrast, the thermodynamic properties of a racemic mixture are not necessarily identical to those of the pure R and S fluids. In fact the excess properties of racemic mixtures have been measured experimentally. However, the excess properties of racemic mixtures tend to be quite small, so that these types of mixtures are a good example of quasi-ideal mixtures [13–19].

We should mention an issue that is of relevance when studying racemic mixtures. In principle, enantiomer R can be converted into enantiomer S according to the reaction:

$$\mathrm{R} \rightleftharpoons \mathrm{S}. \tag{1}$$

Therefore, since interconversion between the two types of molecule is possible they must be in chemical equilibrium. When simulating racemic mixtures one should consider the possibility of trial moves that change the chemical identity of the molecule. That will guarantee that the system is in chemical equilibrium. Therefore, rigorously, for a mixture of enantiomers R and S, composition is not an independent variable, since for a certain temperature and pressure the composition of the system is given by the condition of chemical equilibrium between the two species. One can buy from a chemical company a bottle with the pure R enantiomer and store this product as pure R for years. The reason is kinetics. The interconversion of R into S may have a very large energetic barrier, so that it may occur at practically zero rate at room temperature (although the presence of acids or other substances may significantly decrease the height of the barrier). If the energetic barrier for the interconversion between R and S species is high, then one can disregard the chemical reaction illustrated by equation (1), and treat components R and S as two independent substances. In that case, for a given temperature and pressure, one must also specify the composition of the system (for instance the molar fraction of isomer R). In fact it is possible to prepare mixtures of isomers R and S with arbitrary composition by mixing the pure R and S at will, provided that the energetic barrier for interconversion is large. Rigorously speaking, to measure excess properties in mixtures of enantiomers, one requires that the reaction of equation (1) does not take place (so that the properties of the pure R and S isomers can be determined experimentally). This is usually (but not always) the case, since the interconversion of R into S requires the

breaking of bonds and usually this is a process with a high activation energy.

Therefore, we shall not include in the present study the possibility of chemical conversion between the isomers (the reaction illustrated by equation (1)). As a consequence, in our simulations the numbers of molecules of type R and S will be fixed, and no attempt will be made to change it during the run. We shall treat the two optical isomers as the two independent components of an ordinary mixture, so that for a given temperature and pressure we need also to specify the composition of the system.

A racemic mixture where the reaction given by equation (1) is not included and/or considered will be denoted a non-reactive racemic mixture. A system of chiral molecules, where the reaction given by equation (1) is considered will be denoted a reactive chiral system. Thus, in this paper we shall focus on non-reactive mixtures of chiral compounds.

Non-reactive mixtures of chiral compounds share a number of similarities with Lennard-Jones symmetric mixtures, which consist of mixtures of spherical LJ molecules, where interactions between particles of type A, and interactions between particles of type B are identical, but the A–B interaction differs from the A–A interaction. These kinds of mixture have been studied in detail by Fan *et al.* [28], de Miguel *et al.* [29] and Vlot *et al.* [23].

In addition to the hard primitive model we shall also consider a system with attractive forces. This model will be denoted the Lennard-Jones primitive model (LJPM). The LJPM is identical to the HPM. Bond lengths, angles, and the location of the interaction sites are coincident with those of the HPM. The only difference is that the hard interaction is replaced by a Lennard-Jones interaction given by

$$U_{ij} = 4\varepsilon_{ij}\left(\left(\frac{\sigma_{ij}}{r_{ij}}\right)^{12} - \left(\frac{\sigma_{ij}}{r_{ij}}\right)^{6}\right). \tag{2}$$

We shall use Lorentz–Berthelot [30] rules for cross interactions so that σ_{ij} and ε_{ij} are given by

$$\sigma_{ij} = \frac{\sigma_{ii} + \sigma_{jj}}{2}, \tag{3}$$

$$\varepsilon_{ij} = [\varepsilon_{ii}\varepsilon_{jj}]^{1/2}. \tag{4}$$

The choice for σ_{ii} and ε_{ii} is as follows. For σ_{ii} we shall choose the same values as for the hard sphere model, so that $\sigma_{11} = 1$, $\sigma_{22} = 0.9$, $\sigma_{33} = 0.8$, $\sigma_{44} = 0.7$, $\sigma_{55} = 0.6$. For ε_{ii} we shall use the simple prescription $\varepsilon_{ii} = \sigma_{ii}$ (apart from units).

Now we shall present the details of the computer simulations performed in this work.

2.2. *Computer simulations details*

To study the racemic mixtures and the optically active pure components we performed Monte Carlo simulations in the *NpT* ensemble [31]. We used 256 molecules, and our runs typically consisted of 120 000 cycles for equilibration followed by 120 000 cycles to determine ensemble averages. A cycle consisted of a trial move per particle, plus a trial volume change for the system. The trial move of a particle was selected with equal probability to be a translation move or a rotation move. In the rotational move a direction is selected randomly and the molecule is rotated by a random angle around the chosen direction. Acceptance probabilities for translation, rotation or volume changes were kept around 40%. Simulations started at low densities (pressures), by locating the molecules on a α-N_2 cubic lattice structure. This structure spontaneously melted at low pressures. Then we gradually increased the pressure and proceeded to obtain the equation of state (EOS) via compression runs. We used the final configuration of a certain run as the initial configuration for the next run. Our simulation box was cubic, and volume changes were performed isotropically so that the simulation box remained cubic through all the runs. In the case of the hard primitive model, two independent runs were performed both for the pure R isomer and for the racemic mixture. The results presented here for the HPM correspond to the average of the results of two independent runs. Since the system consists of hard interactions, temperature is not a relevant variable. Pressures and densities will be given in reduced units:

$$p^* = p/(kT/\sigma_{11}^3), \tag{5}$$

$$\rho^* = \rho\sigma_{11}^3, \tag{6}$$

where σ_{11} is the diameter of the central atom, p is the pressure and $\rho = N/V$ is the number density of the systems (number of molecules per unit volume). For a certain reduced pressure the output of the simulation is the reduced density.

In addition to the EOS, we computed also the site–site pair correlation functions between sites. The site–site correlation functions are denoted as g_{ij}^{AB} where $i, j \in 1$, 2, 3, 4, 5 and $A, B \in R, S$. For instance g_{11}^{RR} denotes the site–site correlation function between site 1 of molecule of type R and site 1 of a molecule of type R. Similarly, g_{11}^{RS} denotes the site–site correlation function between site 1 of molecule R and site 1 of molecule S. The number assigned to each of the atoms of the molecule is presented in tables 1 and 2. For determining g_{ij}^{AB} we used *NVT* simulations. The site–site correlation function is calculated in the *NVT* ensemble as [32]

$$g_{ij}^{RS}(r) = f\frac{\langle N_{ij}^{RS}(r)\rangle}{N_R\rho_S V(r)}, \quad (7)$$

$$g_{ij}^{RR}(r) = f\frac{\langle N_{ij}^{RR}(r)\rangle}{N_R\rho_R V(r)}, \quad (8)$$

where $V(r)$ is the volume of the spherical cell with r between $r-\delta r/2$ and $r+\delta r/2$, N_A is the number of particles of type A, ρ_B is the number density of molecules of type B, $\langle N_{ij}^{AB}(r)\rangle$ is the average number of pairs of sites of type i for molecule A, and j for molecule B, with distances between $r-\delta r/2$ and $r+\delta r/2$. The factor f is two when A = B and one when A ≠ B. In this work (unless other choice is indicated) we used $\delta r = 0.02\sigma_{11}$. Note that at large distances the site–site correlation function in the NVT ensemble goes to one for g_{ij}^{AB} (with A different from B), but goes to $1-1/N_A$ for g_{ij}^{AA}. We checked our subroutines for the evaluation of g_{ij} by comparing the results of our program with those of a number of mixtures of hard bodies, obtaining good agreement in all cases [33].

In addition to the simulations for the HPM we also performed simulations for the LJPM, and the details are totally analogous to those described previously. The values of the central atom, 1, were used for obtaining reduced units. For the LJPM, the reduced density, pressure, temperature and energy are given by

$$\rho^* = \rho\sigma_{11}^3, \quad (9)$$

$$p^* = p/(kT/\sigma_{11}^3), \quad (10)$$

$$T^* = T/(\varepsilon_{11}/k), \quad (11)$$

$$U^* = U/(N\varepsilon_{11}). \quad (12)$$

All simulations of the LJPM were performed at the reduced temperature $T^* = 4$. Clearly this temperature is above the critical temperature of the pure enantiomers. By choosing this rather high temperature we avoid the complication of the appearance of vapour–liquid phase separation in the system. In the simulations of the LJPM, each site–site interaction was truncated (but not shifted) at $r_c/\sigma_{11} = 3$. Therefore all site–site interactions are truncated at the same distance. A long range correction to the energy was added assuming $g_{ij} = 1$ beyond the cutoff value. Therefore the total value of the long range correction to the internal energy is given by

$$\frac{U_{lrc}}{N} = \frac{\rho}{2}\sum_A\sum_B x_A x_B \sum_{i\in A}\sum_{j\in B}\varepsilon_{ij}16\pi\frac{\sigma_{ij}^3}{3}\left(\frac{1}{3}\left(\frac{\sigma_{ij}}{r_c}\right)^9 - \left(\frac{\sigma_{ij}}{r_c}\right)^3\right), \quad (13)$$

where x_A is the mole fraction of enantiomer A, x_B is the mole fraction of enantiomer B, i denotes the sites of enantiomer A, and j denotes the sites of enantiomer B. Note that the long range correction is density dependent. Therefore the long range correction must be included within the Markov chain of the NpT simulations (i.e. when attempting a volume change the long range correction must be included for the actual density and for the trial density, and this change of energy must be included within the acceptance criterion). Simulations of the LJPM are considerably more time consuming than those of the HPM. Therefore, only one run was performed for the pure R fluid and for the racemic mixture.

Before finishing we should mention an aspect of the simulations to be considered when studying racemic mixtures. The mixing of components R and S within the mixture must be good. By good mixing we mean that components R and S should be homogeneously distributed within the simulation box. Otherwise wrong results and conclusions (thermodynamic and structural) can be obtained from the simulations. To obtain good mixing two actions were taken. The first is that in the intial low density configuration the R and S molecules are distributed homogeneously within the solid α–N_2 solid structure. The second is that in addition to the usual translation and rotation moves, a new type of Monte Carlo move is included within the simulations. We denote this move the exchange move [34]. In an exchange move an R and an S molecule is each selected randomly within the mixture. Then the positions of the two molecules are exchanged. The exchange move is used only to achieve good mixing, especially at high densities, but this move does not change the composition, and therefore does not account for the chemical reaction represented by equation (1). To include equation (1) within the simulations, one should randomly select one, and only one, molecule (either R and S) and change its chemical identity (from R to S or from S to R). This is equivalent to regarding the two enantiomers R and S as two different states of the same type of molecule, and the change of identity corresponds to the sampling of an 'internal' degree of freedom. Note that in this case the number of R or S molecules is not conserved during the simulation run. This is one way to include the reaction given by equation (1) within the simulations. However, this has not been done in the present work. As mentioned above, we shall assume that there is a large energy barrier between isomers R and S, so that there is no mutual conversion, and we can regard the mixture as a standard mixture of two different components (for example Ar and N_2). The exchange move included within the runs was chosen in order to achieve mixing, and not to account for the possibility of a chemical reaction like that given by equation (1).

When choosing a trial move for a molecule in the racemic mixture we may select translation, rotation and exchange moves, with probabilities of 0.4, 0.4 and 0.2, respectively. Typical acceptance ratios for exchange moves ranged from almost 100% at very low densities to 0.3% at the highest densities considered. These acceptance ratios are sufficient to guarantee good mixing of the R and S enantiomers.

2.3. *Virial coefficients for the hard model*

At low densities the compressibilty factor can be expanded in powers of the density:

$$Z = \frac{p}{\rho kT} = 1 + B_2\rho + B_3\rho^2 + B_4\rho^3 + \cdots. \tag{14}$$

For a hard model one can define the volume fraction y as

$$y = \rho V_{\mathrm{m}}, \tag{15}$$

where V_{M} is the molecular volume. For the HPM the molecular volume is given by

$$V_{\mathrm{m}} = \frac{\pi}{6}\sigma_{11}^3(1 + 0.9^3 + 0.8^3 + 0.7^3 + 0.6^3) = 1.466\,08. \tag{16}$$

The virial expansion can be written as:

$$Z = \frac{p}{\rho kT} = 1 + B_2^* y + B_3^* y^2 + B_4^* y^3 + \cdots, \tag{17}$$

where the reduced virial coefficients B_i^* are defined as $B_i^* = B_i / V_{\mathrm{m}}^{(i-1)}$. For a binary system, for example that of the racemic mixture,the reduced virial coefficients can be expressed as

$$B_2^* = \sum_{\mathrm{A}}\sum_{\mathrm{B}} x_{\mathrm{A}} x_{\mathrm{B}} B_{\mathrm{AB}}^*, \tag{18}$$

$$B_3^* = \sum_{\mathrm{A}}\sum_{\mathrm{B}}\sum_{\mathrm{C}} x_{\mathrm{A}} x_{\mathrm{B}} x_{\mathrm{C}} B_{\mathrm{ABC}}^*, \tag{19}$$

$$B_4^* = \sum_{\mathrm{A}}\sum_{\mathrm{B}}\sum_{\mathrm{C}}\sum_{\mathrm{C}} x_{\mathrm{A}} x_{\mathrm{B}} x_{\mathrm{C}} x_{\mathrm{D}} B_{\mathrm{ABCD}}^*, \tag{20}$$

where x_{A} denotes the molar fraction of component A, and the capital letters A, B, C, D may adopt any of the two values R for the R enantiomer, or S for the S enantiomer. Therefore, the second virial coefficient B_2^* can be determined if B_{RR}^*, B_{SS}^*, and B_{RS}^* are known. By symmetry it must hold that $B_{\mathrm{RR}}^* = B_{\mathrm{SS}}^*$. However, B_{RS}^* is not necessarily identical to B_{RR}^*. Similarly, to obtain the third virial coefficient B_3^*, the coefficients B_{RRR}^*, B_{RRS}^*, B_{RSS}^*, and B_{SSS}^* must be determined. By symmetry considerations it must hold that $B_{\mathrm{RRR}}^* = B_{\mathrm{SSS}}^*$ and $B_{\mathrm{RRS}}^* = B_{\mathrm{SSR}}^*$. In principle, B_{RRR}^* and B_{RRS}^* are not equal. For the fourth virial coefficient, one must determine $B_{\mathrm{RRRR}}^* = B_{\mathrm{SSSS}}^*$, $B_{\mathrm{RRRS}}^* = B_{\mathrm{SSSR}}^*$, and $B_{\mathrm{RRSS}}^* = B_{\mathrm{SSRR}}^*$, so there are only three different independent contributions. Therefore, to determine B_2, B_3 and B_4 for the mixture one must first compute B_{RR}, B_{RS}, B_{RRR}, B_{RRS}, R_{RRRR}, B_{RRRS} and B_{RRSS}. To determine those coefficients we used the method proposed by Ree and Hoover [35], as extended to non-spherical systems by Rigby [36]. The procedure and graphs that must be evaluated in order to determine those coefficients have been described in detail in [37, 38]. We used five independent determinations to compute these virial coefficients, and the results reported here are the average of these five independent determinations. In each determination we used $N_{\mathrm{orien}} = 100\,000$ and $N_{\mathrm{chemical}} = 2000$, where the meanings of the parameters N_{orien} and N_{chemical} were given in [37].

2.4. *Bonded hard sphere theory for the hard primitive model of a chiral molecule*

In addition to the virial calculations and the computer simulations described above we have determined the EOS of the HPM theoretically using the bonded hard sphere implementation of Wertheim's theory [5, 39–43] as proposed by Archer, Amos and Jackson [44–46]. This theory is quite suitable for describing the EOS of a system formed by tangent hard spheres. Therefore, it can be used for describing the HPM model proposed in this work. We shall describe the implementation of the BHS for a pure fluid (say the R enantiomer). The bonded hard sphere model starts from the reference system of unassociated sites and evaluates the effect of bonding on the EOS. The EOS of the BHS for the HPM model is given by

$$Z = 5Z_{\mathrm{hs}} - \sum_{\mathrm{bonds}}\left[1 + \frac{\rho}{g_{ij}^{\mathrm{hs}}(\sigma_{ij})}\left(\frac{\partial g_{ij}^{\mathrm{hs}}(\sigma_{ij})}{\partial\rho}\right)_{\mathrm{TN}}\right], \tag{21}$$

where the factor 5 is due to the fact that the molecule (say enantiomer R) breaks into five different monomers. The sum in equation (21) runs over all bonds formed in the molecule. For the R enantiomer, the bonds of the molecule are those formed between sites 1–2, 1–3, 1–4 and 1–5. The compressibility factor of the reference system of unbonded hard spheres Z_{hs} is described by the Boublik–Mansoori–Carnahan–Starling–Leland EOS [47, 48], which is given by

$$Z_{\mathrm{hs}} = \frac{6}{\pi\rho}\left[\frac{\zeta_0}{1-\zeta_3} + \frac{3\zeta_1\zeta_2}{(1-\zeta_3)^2} + \frac{3\zeta_2^3}{(1-\zeta_3)^3} - \frac{\zeta_3\zeta_2^3}{(1-\zeta_3)^3}\right], \tag{22}$$

where the variable ζ_l is defined as

$$\zeta_l = \frac{\pi\rho}{6}\left[\sum_i x_i \sigma_{ii}^l\right], \tag{23}$$

with x_i the molar fraction of atoms of type i in the unbounded mixture. The contact value for the pair correlation function between sites in the reference unbonded system and its derivative (with respect to the total number of monomers) are given by [46, 47]

$$g_{ij}^{\mathrm{hs}}(\sigma_{ij}) = \frac{1}{1-\zeta_3} + 3\left(\frac{\sigma_i\sigma_j}{\sigma_i+\sigma_j}\right)\frac{\zeta_2}{(1-\zeta_3)^2} + 2\left(\frac{\sigma_i\sigma_j}{\sigma_i+\sigma_j}\right)^2\frac{\zeta_2^2}{(1-\zeta_3)^3}, \tag{24}$$

$$\left(\rho\frac{\partial g_{ij}^{\mathrm{hs}}(\sigma_{ij})}{\partial\rho}\right)_{\mathrm{TN}} = \frac{\zeta_3}{(1-\zeta_3)^2} + 3\left(\frac{\sigma_i\sigma_j}{\sigma_i+\sigma_j}\right)\frac{\zeta_2(1+\zeta_3)}{(1-\zeta_3)^3} + 2\left(\frac{\sigma_i\sigma_j}{\sigma_i+\sigma_j}\right)^2\frac{\zeta_2^2(2+\zeta_3)}{(1-\zeta_3)^4}, \tag{25}$$

where $\sigma_{ij} = (\sigma_{ii}+\sigma_{jj})/2$.

According to the BHS the equation of state for pure R is identical to that of the pure S enantiomer (as it should be). The BHS has been extended to mixtures, and the details are given in [46]. In the particular case of racemic mixtures, it turns out that the diameters of the sites and the types of contact are identical for the R and S isomers. Therefore, BHS theory predicts the same EOS for the pure components and for the racemic mixture. This is an important and interesting result. It means that according to the BHS the excess volume of a racemic mixture is zero.

2.5. *Wertheim's theory for the Lennard-Jones primitive model of a chiral molecule*

According to Wertheim's first-order perturbation theory (TPT1) the residual free energy, compressibility factor and residual internal energy of the pure R enantiomer are given by [9, 49]

$$\frac{A_{\mathrm{res}}}{NkT} = 5\frac{A_{\mathrm{res}}^{\mathrm{mix}}}{N_{\mathrm{mono}}kT} - \sum_{j=2}^{5}\ln y_{1j}(\sigma_{1j}), \tag{26}$$

$$Z = 5Z^{\mathrm{mix}} - \sum_{j=2}^{5}\left[1+\rho\frac{\partial}{\partial\rho}\ln y_{1j}(\sigma_{1j})\right], \tag{27}$$

$$\frac{U_{\mathrm{res}}}{NkT} = 5\frac{U_{\mathrm{res}}^{\mathrm{mix}}}{N_{\mathrm{mono}}kT} + \sum_{j=2}^{5}\left[T\frac{\partial}{\partial T}\ln y_{1j}(\sigma_{1j})\right], \tag{28}$$

where the superscript mix denotes properties of the reference system of unbonded monomers and y_{ij} is the background correlation function of the mixture of unbonded monomers. The number of unbonded monomers is (obviously) $5N$. There is no distinction between $y_{ij}(\sigma_{ij})$ and $g_{ij}(\sigma_{ij})$, since the LJ pair potential vanishes when $r_{ij} = \sigma_{ij}$.

The properties of the reference system of LJ unbonded monomers are unknown. At this point we shall use the one-fluid approximation which, as illustrated by Blas and Vega [49], yields quite good results for heteronuclear LJ chains. In the one-fluid theory the parameters ε_x and σ_x of the equivalent LJ one-fluid system are defined as [50]

$$\sigma_x^3 = \sum_i\sum_j x_i x_j\sigma_{ij}^3, \tag{29}$$

$$\varepsilon_x\sigma_x^3 = \sum_i\sum_j x_i x_j\sigma_{ij}^3\varepsilon_{ij}, \tag{30}$$

where x_i is the molar fraction of sites of type i. In our case the molecule is formed by five different types of site so that $x_i = 0.2$ for all of them. When the one-fluid mixing rules are applied to the LJ model of this work it yields $\varepsilon_x/\varepsilon_{11} = 0.830\,20$ and $\sigma_x/\sigma_{11} = 0.812\,31$.

Therefore the residual free energy of the reference unbonded LJ system (formed by 5 different types of monomer site) is approximated to that of a pure LJ fluid with parameters ε_x and σ_x:

$$\frac{A_{\mathrm{res}}^{\mathrm{mix}}}{N_{\mathrm{mono}}kT} = \frac{A_{\mathrm{res}}^{\mathrm{lf}}}{N_{\mathrm{mono}}kT}. \tag{31}$$

Similarly we shall assume that

$$y_{ij}(\sigma_{ij}) = y_{1\mathrm{f}}(\sigma_x). \tag{32}$$

It is important to mention that the properties of the left and right hand sides are evaluated at the same absolute temperature and number density for the reference system of unbonded monomers and for the equivalent one-fluid system. However, note that the same absolute temperature corresponds to two different reduced temperatures in the left and right hand sides, and that the same number density corresponds to different reduced densities in the left and right hand sides. In fact, properties on the left hand side correspond to a reduced number density of monomers of $5\rho^*$ and to a reduced temperature of T^*, whereas on the right hand side they correspond to $5\rho_x^*$ and T_x^*, where we have defined ρ_x^* as

$$\rho_x^* = \rho\sigma_x^3 \tag{33}$$

and

$$T_x^* = T/(\varepsilon_x/k). \tag{34}$$

By using equations (26)–(34) along with the parametrization of the properties of the LJ fluid (free energy and y_{ij}) performed by Johnson, Muller and Gubbins [9, 51] the properties of the pure R isomer are obtained readily. Note that some care is needed when using this correla-

tion at very low densities [52]. Obviously the properties of the pure R isomer are identical to those of the S isomer. The same is true for the racemic mixture, since TPT1 does not distinguish between the optical isomers. Therefore, according to TPT1, the properties of the pure isomers and those of the racemic mixture are indistinguishable.

3. Results

3.1. *Results for the hard primitive model*

Before presenting the results for the chiral HPM let us discuss the results for two other models for which simulations were performed in order to test the Monte Carlo program. First of all we performed simulations for the tetrahedral (non-chiral) model proposed by Abascal and Bresme [53]. We found good agreement between our results and those reported by Abascal and Bresme. We then performed simulations for a tetrahedral model (non-chiral) formed by a central sphere of diameter unity, and four tangent spheres of diameter unity, tangent to the central sphere, and arranged in a tetrahedral coordination. This model, presented in figure 1 (*b*), was first proposed by Sear *et al.* [54], and we shall refer to it as the Sear–Amos–Jackson model. In table 3 the simulations results for the Sear–Amos–Jackson model obtained in this work are presented. These results were obtained by using 108 particles and runs consisting of 60 000 cycles for equilibration and 60 000 cycles for averages. In the same table we have included the simulation results of Sear *et al.* Both sets of data are compared with each other and with the results from BHS theory (figure 2). As can be seen, our results are in good agreement with the results of Sear *et al.* at low and medium densities (up to a reduced pressure of 3.6), but at high densities we obtain higher densities (for a given pressure). The results of Sear *et al.* were obtained from *NpT* simulations using a system of 256 particles. We cannot assess the origin of the discrepancy between our data and those of Sear *et al.* for high pressures. Our data seem to be closer to BHS theory than those of Sear *et al.*, but this is not a guarantee of accuracy. We repeated the calculations by using $N = 256$ molecules (instead of 108), and these results are also presented in table 3. The EOS obtained was again coincident with our results for 108 molecules. Note that we used five simulations for increasing the pressure from $p^* = 3.6$ up to $p^* = 6$, whereas this compression was performed in just one simulation by Sear *et al.* In any case we obtained (except for their highest pressure) good agreement with the Sear, Amos and Jackson results.

Table 3. Simulation results for the tetrahedral (non-chiral) model of Sear *et al.* [54]. The model consists of five identical hard spheres: one central and the other four located in tetrahedral coordination, bonded tangentially to the central sphere. The first set of results corresponds to the simulation results of this work. Results below the line are those of Sear *et al.* [54]. The number of molecules used in the simulations is denoted N.

p^*	ρ^*	y	Z	N
0.1	0.040 0	0.104 7	2.500	108
0.3	0.065 9	0.172 5	4.552	108
0.5	0.081 2	0.212 6	6.157	108
0.7	0.091 3	0.239 0	7.667	108
0.9	0.099 8	0.261 3	9.018	108
1.1	0.108 1	0.283 0	10.175	108
1.6	0.120 7	0.316 0	13.256	108
2.1	0.130 3	0.341 1	16.116	108
2.6	0.138 7	0.363 1	18.745	108
3.1	0.145 2	0.380 1	21.349	108
3.6	0.150 4	0.393 7	23.936	108
4.1	0.155 4	0.406 8	26.383	108
4.6	0.161 5	0.422 8	28.483	108
5.1	0.164 7	0.431 2	30.965	108
5.6	0.168 6	0.441 4	33.214	108
6.1	0.171 2	0.448 2	35.630	108
0.1	0.039 79	0.104 17	2.513	256
0.3	0.066 11	0.173 08	4.537	256
0.5	0.081 57	0.213 55	6.129	256
0.7	0.091 19	0.238 73	7.676	256
0.9	0.099 56	0.260 65	9.039	256
1.1	0.107 17	0.280 57	10.264	256
1.6	0.121 67	0.318 53	13.150	256
2.1	0.131 24	0.343 59	16.001	256
2.6	0.138 95	0.363 77	18.711	256
3.1	0.145 69	0.381 42	21.278	256
3.6	0.150 76	0.394 69	23.879	256
4.1	0.156 43	0.409 53	26.209	256
4.6	0.162 36	0.425 03	28.333	256
5.1	0.165 15	0.432 36	30.881	256
5.6	0.168 87	0.442 10	33.161	256
6.1	0.171 91	0.450 06	35.483	256
0.094 862 903	0.039 038 232	0.102	2.43	256
0.213 443 97	0.057 687 559	0.151	3.70	256
0.418 312 67	0.075 236 091	0.197	5.56	256
0.758 386 04	0.094 326 621	0.247	8.04	256
1.309 991 6	0.113 419 19	0.297	11.55	256
2.194 600 2	0.130 243 34	0.341	16.85	256
3.610 340 8	0.147 060 72	0.385	24.55	256
5.889 967 9	0.160 445 87	0.420	36.71	256

Now we shall present the results for the primitive model of a chiral molecule HPM. In table 4 the simulations results for the pure R enantiomer are presented and in table 5 those for the racemic mixture (with 50% R and 50% S). Figure 3 gives the EOS as obtained from simulations of the pure fluid and of the racemic mixture. The BHS theory results are shown also. First we see that the BHS describes the simulation data quite

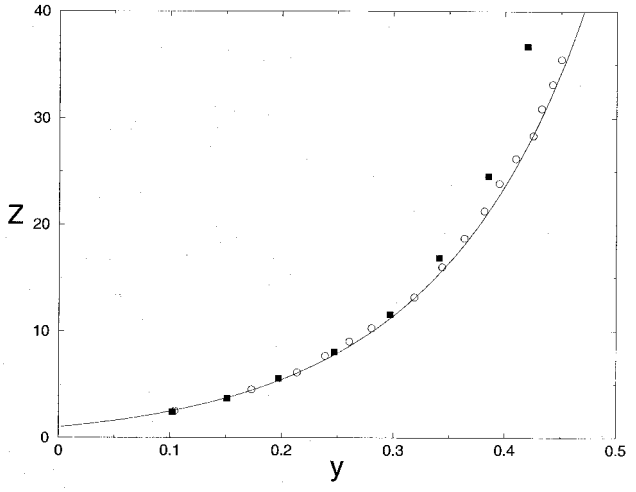

Figure 2. EOS of the tetrahedral model of figure 1 (*b*) line, results from BHS theory; circles, results from the *NpT* simulations of this work; and squares, results from *NpT* simulations of Sear *et al.* [54].

well up to high densities. Therefore, it seems a suitable theory for describing the EOS of systems similar to those considered in this work. Second, as can be seen in figure 3 the EOS of the pure fluid and that of the racemic mixture are similar and any differences between the two systems fall within the error bars. A careful inspection to tables 4 and 5 reveals that in some cases for a given pressure the density of the racemic mixture is higher than that of the pure R isomer, whereas for a slightly higher or lower pressure the opposite is true. This indicates that differences between the two models are smaller than the statistical error associated with our simulations. We again recall that the data of tables 4 and 5 correspond to the averages of two independent runs. We conclude that we do not observe significant differences in the EOS between the pure R isomer and the racemic mixture, and if differences exist then they are smaller than the statistical error associated with our simulations. The only exception to this is the behaviour at the highest densities, where we observe differences between the pure enantiomer and that of the racemic mixture. In fact the racemic mixture seems to have a higher density than the pure enantiomer. It seems that the racemic mixtures show better packing of the molecules at very high pressures (or densities). In fact we have performed five independent runs, for $p^* = 12.10$, for the pure R enantiomer and for the racemic mixture (table 6), and the density of the racemic mixture is higher than that of the pure R enantiomer. The average density is presented in the final row of table 6. The average volume fraction obtained at this pressure is $y = 0.4760$ for the pure R fluid and $y = 0.4800$ for the racemic mixture, so differences are about 0.8%, and are significant. However, the volume fraction for this pressure is quite high, and it is not clear whether we are in a metastable region of the fluid branch for the model considered (i.e. the fluid–solid equilibrium may have occurred at a lower density).

Table 4. *NpT* simulation results for the R enantiomer of the HPM model of this work. Results correspond to the average of two independent runs with $N = 256$, 120 000 cycles for equilibration, and 120 000 cycles for obtaining averages.

p^*	ρ^*	y	Z
0.10	0.052 70	0.077 26	1.897
0.20	0.077 43	0.113 52	2.582
0.30	0.094 48	0.138 51	3.175
0.50	0.118 67	0.173 97	4.213
0.70	0.137 02	0.200 88	5.108
0.90	0.150 94	0.221 29	5.962
1.10	0.163 11	0.239 14	6.743
1.40	0.176 43	0.258 66	7.935
1.60	0.185 35	0.271 74	8.632
2.10	0.202 45	0.296 80	10.373
2.60	0.217 16	0.318 36	11.973
3.10	0.229 14	0.335 93	13.529
3.60	0.240 70	0.352 89	14.956
4.10	0.247 94	0.363 51	16.536
4.60	0.257 36	0.377 31	17.873
5.10	0.264 43	0.387 69	19.286
5.60	0.270 73	0.396 91	20.684
6.10	0.276 57	0.405 47	22.055
6.60	0.283 30	0.415 34	23.296
7.10	0.288 17	0.422 48	24.638
7.60	0.292 21	0.428 40	26.008
8.10	0.298 26	0.437 27	27.157
8.60	0.302 65	0.443 70	28.415
9.10	0.307 74	0.451 18	29.569
9.60	0.310 93	0.455 84	30.875
10.10	0.313 19	0.459 16	32.248
11.10	0.318 42	0.466 83	34.859
11.60	0.321 33	0.471 09	36.099
12.10	0.324 53	0.475 78	37.284
12.60	0.325 70	0.477 51	38.685
13.10	0.327 75	0.480 50	39.970

Now let us focus on the structural results (namely the site–site correlation functions). First we introduced a consistency check. In the *NpT* simulations pressure is imposed on the system. The output of the simulations is the average density. From the imposed pressure and the density obtained one can compute the compressibility factor. However, the compressibility factor can be obtained within the run also by using the virial theorem. According to the virial theorem the compressibility factor of a pure fluid (say the R isomer) can be obtained from the expression [27]

Table 5. *NpT* simulation results for the racemic mixture of the HPM model of this work. Results correspond to the average of two independent runs with $N = 256$, 120 000 cycles for equilibration, and 120 000 cycles for obtaining averages.

p^*	ρ^*	y	Z
0.10	0.052 40	0.076 82	1.908
0.20	0.077 62	0.113 80	2.576
0.30	0.094 14	0.138 02	3.186
0.50	0.119 27	0.174 86	4.192
0.70	0.136 54	0.200 18	5.126
0.90	0.150 77	0.221 03	5.969
1.10	0.162 08	0.237 63	6.786
1.40	0.177 57	0.260 33	7.884
1.60	0.185 19	0.271 49	8.640
2.10	0.202 30	0.296 58	10.380
2.60	0.216 34	0.317 18	12.018
3.10	0.228 96	0.335 68	13.539
3.60	0.238 67	0.349 91	15.083
4.10	0.248 25	0.363 97	16.515
4.60	0.256 53	0.376 09	17.931
5.10	0.263 95	0.386 98	19.321
5.60	0.270 26	0.396 22	20.720
6.10	0.276 34	0.405 14	22.074
6.60	0.282 28	0.413 85	23.381
7.10	0.288 99	0.423 68	24.568
7.60	0.292 99	0.429 54	25.939
8.10	0.297 53	0.436 20	27.224
8.60	0.302 32	0.443 22	28.446
9.10	0.306 22	0.448 94	29.717
9.60	0.310 86	0.455 74	30.882
10.10	0.313 66	0.459 85	32.200
11.10	0.320 65	0.470 10	34.617
11.60	0.322 82	0.473 28	35.934
12.10	0.327 42	0.480 02	36.956
12.60	0.329 48	0.483 05	38.241
13.10	0.332 70	0.487 76	39.374

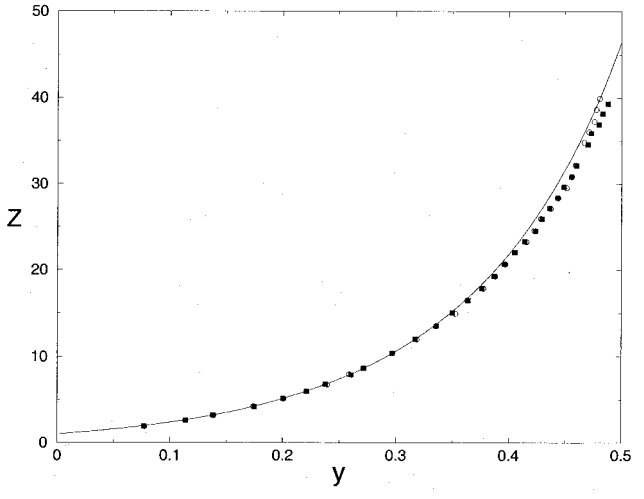

Figure 3. EOS for the HPM of this work: circles, results for the pure R enantiomer; squares, results for the racemic mixture; and line, results from BHS theory.

Table 6. *NpT* simulations results with $N = 256$ molecules for the HPM of this work with $p^* = 12.10$. Results are presented for five independent runs of the pure R enantiomer ρ^*_R and for the racemic mixture ρ^*_{RS}. In the last row is the average density from these independent runs.

ρ^*_R	ρ^*_{RS}
0.324 92	0.327 59
0.324 49	0.326 82
0.325 08	0.327 31
0.324 54	0.327 27
0.324 60	0.328 00
0.324 7	0.327 4

$$\frac{\beta P}{\rho} = 1 + \frac{2}{3}\pi\rho \sum_{\alpha\beta} \sigma^2_{\alpha\beta} g_{\alpha\beta}(\sigma_{\alpha\beta}) \langle \mathbf{r}_{12} \cdot \mathbf{m}_{\alpha\beta} \rangle_c, \qquad (35)$$

where the sum runs over all pairs of sites in the molecule, $g_{\alpha\beta}(\sigma_{\alpha\beta})$ is the contact value of the pair correlation function between sites α and β, $\mathbf{r}_{12}$ is the vector connecting the reference atoms of the molecule (in this case the central atoms), $\mathbf{m}_{\alpha\beta}$ is a unit vector between site α in molecule 1 and site β in molecule 2, the expression in pointed brackets denotes thermodynamic average, and the subscript c indicates that the bracket is evaluated at contact (i.e. when the two sites α and β are at a distance given by $\sigma_{\alpha\beta}$). Evaluation of the virial for hard bodies requires the evaluation of contact values of the pair correlation function. We evaluated the contact values by extrapolating the required functions to contact at short distances. Table 7 gives all the contact values required to evaluate the virial, for the pure R isomer fluid at $p^* = 1.6$. The value of Z from our *NpT* simulations yields 8.63, whereas the expression from the virial theorem yields 8.59, which is in reasonable agreement. This provides us with confidence in our determination of the pair correlation functions.

As we have shown above, at low and medium pressures the EOS of the racemic mixture is identical (within statistical uncertainty) to that of the pure R fluid. However, at high pressures differences in the EOS between the pure R fluid and the racemic mixture appear.

An interesting issue is whether in the racemic mixture there is any structural difference in the correlation between molecules of type R with respect to crossed correlation between a molecule of type R and another of type S. These site–site correlation functions can be studied, within the racemic mixture, for pairs of molecules of type R to yield the g_{ij}^{RR}, or between a molecule of type R and another of type S to yield g_{ij}^{RS}. The ques-

Table 7. Determination of the pressure by the virial theorem for the pure R isomer of the HPM at $p^* = 1.6$. For each site–site interaction g_{ij} the contact value of the pair correlation function $g_{\alpha\beta}(\sigma_{\alpha\beta})$ and the contact value of the function $\langle \mathbf{r}_{12} \cdot \mathbf{m}_{\alpha\beta} \rangle_c$ (in σ_{11} units) are given. The last column is the multiplicity (i.e. the number of times that this interaction appears in the virial theorem), which is 2 for interactions between different sites and 1 for interactions between the same type of site. The contribution of each interaction to the virial (except by the multiplicity) is given by $\sigma_{\alpha\beta}^2 g_{\alpha\beta}(\sigma_{\alpha\beta}) \langle \mathbf{r}_{12} \cdot \mathbf{m}_{\alpha\beta} \rangle_c$ (see equation (35) of the main text) and this is presented in the fifth column.

Kind	$\sigma_{\alpha\beta}$	$g_{\alpha\beta}(\sigma_{\alpha\beta})$	$\langle \mathbf{r}_{12} \cdot \mathbf{m}_{\alpha\beta} \rangle_c$	Contribution	Multiplicity
g_{11}	1.00	0.02	1.00	0.02	1
g_{12}	0.95	0.60	1.30	0.70	2
g_{22}	0.90	1.70	1.29	1.78	1
g_{13}	0.90	0.63	1.27	0.65	2
g_{23}	0.85	1.51	1.23	1.34	2
g_{33}	0.80	1.40	1.22	1.09	1
g_{14}	0.85	0.65	1.24	0.58	2
g_{24}	0.80	1.38	1.22	1.08	2
g_{34}	0.75	1.30	1.20	0.88	2
g_{44}	0.70	1.25	1.15	0.70	1
g_{15}	0.80	0.65	1.20	0.50	2
g_{25}	0.75	1.28	1.24	0.86	2
g_{35}	0.70	1.29	1.16	0.73	2
g_{45}	0.65	1.12	1.10	0.52	2
g_{55}	0.60	1.10	1.08	0.43	1

tion is to analyse structural differences between different components in the racemic mixture. For that purpose we have decided to study the racemic mixture at two different densities. One corresponds to a low density state $y = 0.1690$ (a reduced pressure of about 0.5) and the second corresponds to a high density state $y = 0.3974$ (a reduced pressure of about 5.6). Simulations were then performed in the NVT ensemble. In order to have good statistics, we performed five independent runs of 400 000 cycles each, with an initial configuration taken from an equilibrated fluid, and we used $\delta r = 0.05\sigma_{11}$ to improve the statistics for g_{ij}. Altogether, these conditions guarantee an uncertainty in g_{ij} for a given value of r of about 0.004. Such high accuracy is needed in order to establish solid conclusions concerning the structural properties of the system.

The g_{11} site–site correlation function is shown at low (figure 4 (*a*)) and at high (figure 4 (*b*)) densities. As can be seen in the racemic mixture, site–site correlation functions between pairs of R molecules and between an R and an S molecule are almost identical. However, small differences are found. In fact the dashed line turns out to be slightly higher than the solid line in figure 4 (*a*, *b*). One striking feature shown in figure 4 is that the solid line is below the dashed line for all distances between the sites. One could be tempted to state that there are small differences between g_{11} for RR correlations and for RS correlations. However, it will be shown now that this is not correct. We have used equations (7) and (8) to compute site–site correlation functions. This is the usual procedure when dealing with mixtures. However, this is not appropriate when dealing with mixtures with components that are almost identical. To illustrate that, let us assume an imaginary binary mixture of hard spheres of diameter 1 for component A and also 1 for component B. Let us assume that half of the molecules are of type A and half of the molecules are of type B. Our binary mixture is indeed a pure hard sphere fluid, but we artificially label the hard spheres of the system as being of type A or of type B. In figure 5 (*a*) the g_{AA} and g_{AB} as obtained from a computer simulation with $N = 256$ and $y = 0.35$ are shown. As can be seen, g_{AB} is slightly higher than g_{AA}. The difference is small but can be seen. On a physical basis g_{AA} and g_{AB} should be identical for this mixture. However, when equations (7) and (8) are used this is not the case. The reason for this discrepancy is that in our imaginary mixture the number of AB pairs is given by $N_A N_B$. However, the number of AA pairs is $N_A(N_A - 1)/2$ and the number of BB pairs is $N_B(N_B - 1)/2$. When using equation (7) for g_{AB} we are using $N_A N_B$ in the denominator. When using equation (8) for g_{AA} we are dividing by $N_A N_A$, and $N_B N_B$ for g_{BB}. This is not fully correct, since it does not correspond to the true number of pairs in the

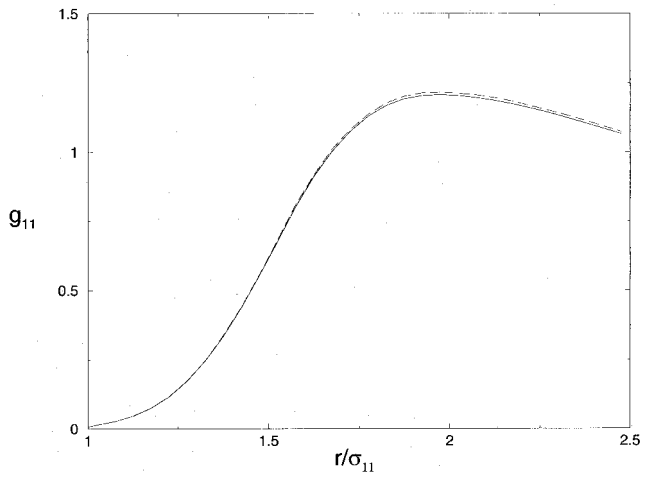

(*a*)

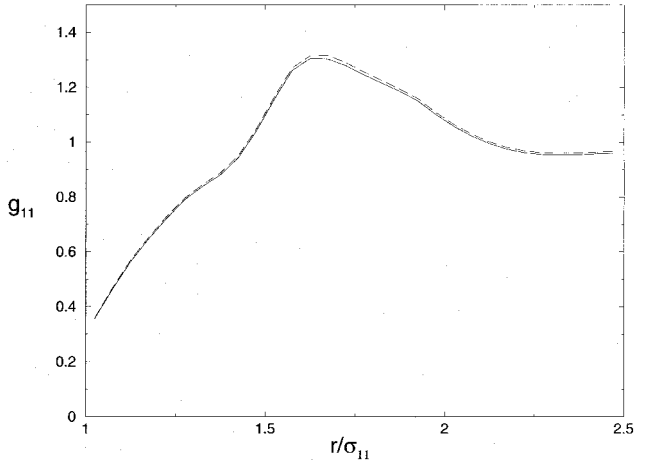

(*b*)

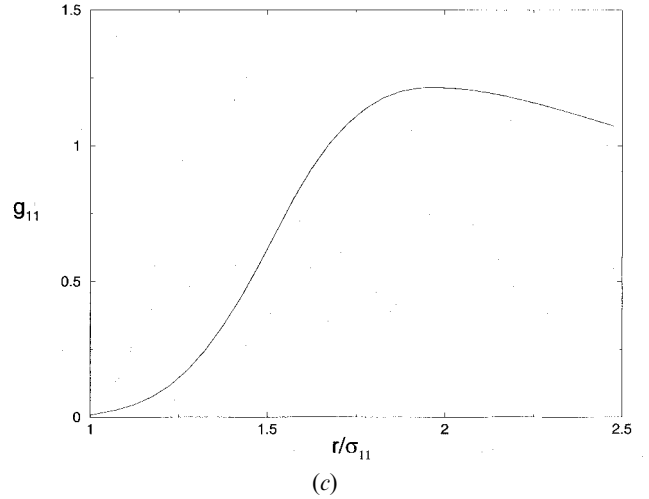

(*c*)

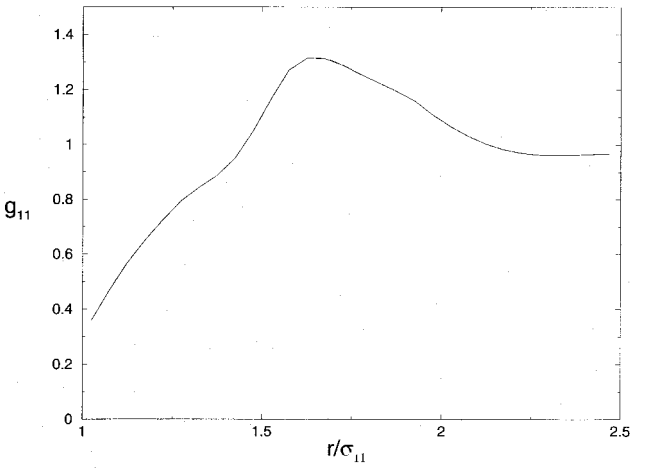

(*d*)

Figure 4. g_{11} in the racemic mixture obtained from the NVT simulations of this work: full line, g_{11}^{RR}; and dashed line, g_{11}^{RS}. (*a*) Results for a low density state with $y = 0.1690$, $\rho^* = 0.115\,28$: g_{11} was obtained using equations (7) and (8) of the main text. (*b*) Results for a high density state with $y = 0.3974$, $\rho^* = 0.271\,06$: g_{11} was obtained using equations (7) and (8) of the main text. (*c*) Results for a low density state with $y = 0.1690$, $\rho^* = 0.115\,28$: g_{11} was obtained using equations (36) and (37) of the main text. (*d*) Results for a high density state with $y = 0.3974$; $\rho^* = 0.271\,06$: g_{11} was obtained using equations (36) and (37) of the main text.

system. In fact the problem can be corrected if the site–site correlation functions are computed from the formulas:

$$g_{ij}^{\mathrm{RS}}(r) = f\frac{\langle N_{ij}^{\mathrm{RS}}(r)\rangle}{N_{\mathrm{R}}\rho_{\mathrm{S}}V(r)}, \tag{36}$$

$$g_{ij}^{\mathrm{RR}}(r) = f\frac{\langle N_{ij}^{\mathrm{RR}}(r)\rangle}{(N_{\mathrm{R}}-1)\rho_{\mathrm{R}}V(r)}. \tag{37}$$

Figure 5 (*b*) shows the site–site correlation functions as obtained by equations (36) and (37) for our imaginary mixture of hard spheres. As can now be seen, g_{AA} and g_{AB} are fully coincident, as they should be. For ordinary mixtures, where component A and B are quite different, the subtle issue of dividing by N_{A} or by $N_{\mathrm{A}} - 1$ in equation (37) will not affect the results significantly. However, for mixtures where structural differences between g_{AA} and g_{AB} are expected to be small, some care should be taken. Therefore, we shall use equations (36) and (37) instead of (7) and (8) to compute site–site correlation functions in this work. Note that for large values of r, g_{ij}^{RS} as given by equation (36) tends to one, whereas g_{ij}^{RR} tends to a value slightly higher than one. In figure 4 (*c*, *d*) the g_{11} function at low and high densities is shown, obtained using equations (36) and (37). As can now be seen, RR and RS correlations are practically identical,

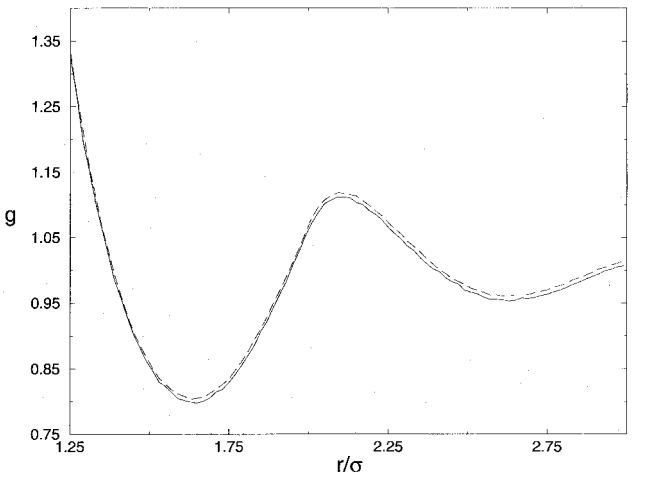

(*a*)

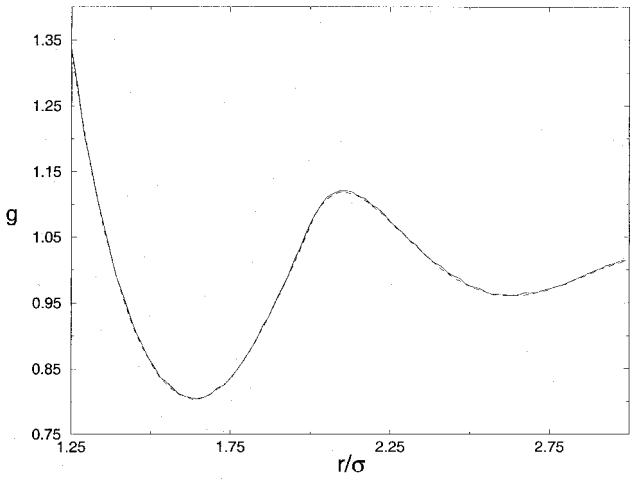

(*b*)

Figure 5. Pair correlation function in a pure hard sphere fluid with $N = 256$, $y = 0.35$ and $\sigma = 1$ (half the molecules are labelled A and the other half B): full line, g_{AA}; dashed line, g_{AB}. For clarity only the region with $r^* > 1.25$ is shown. (*a*) Results when equations (7) and (8) were used to compute g_{AA} and g_{AB}. (*b*) Results when equations (36) and (37) were used to compute g_{AA} and g_{AB}.

and differences fall well below the statistical error of our simulations. Therefore, we conclude that in the racemic mixture no differences are found between RR and RS correlations for g_{11}. In all the simulations of this work we checked that g_{ij}^{RR} and g_{ij}^{SS} were identical in the racemic mixture. This is an exact and obvious result. The fact that we reproduced this result is a guarantee of good equilibration in the racemic mixture. However, our finding that g_{ij}^{RR} and g_{ij}^{RS} are also identical is an unexpected result whose explanation does not seem obvious at all. Let us now present structural results for other correlation functions in the racemic mixture to see whether this surprising result also holds for other site–site correlation functions.

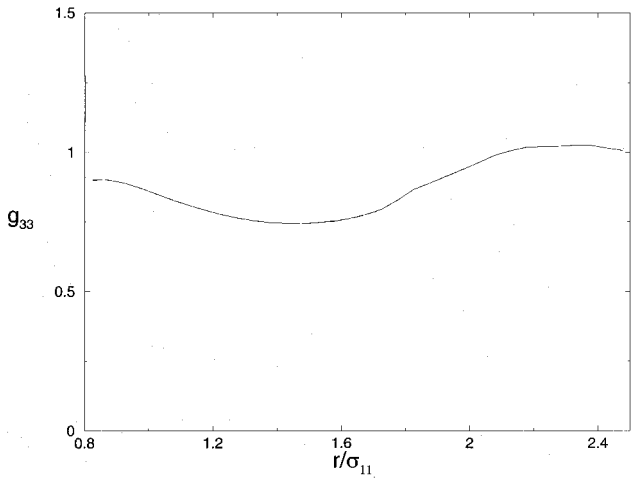

(*a*)

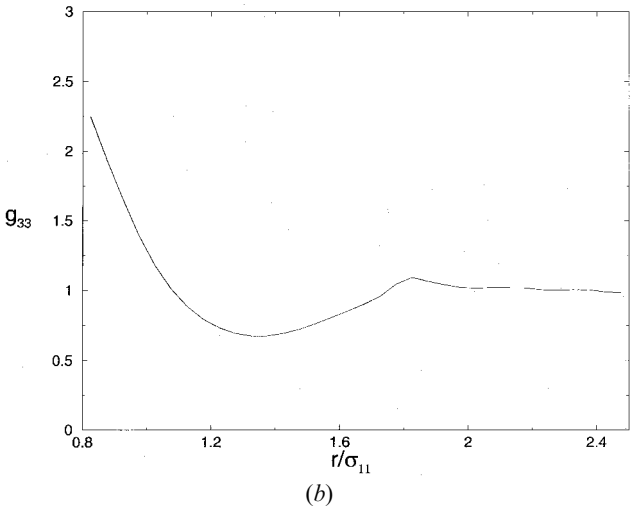

(*b*)

Figure 6. g_{33} in the racemic mixture obtained from the NVT simulations of this work: full line, g_{33}^{RR}; dashed line, g_{33}^{RS}. Note that the full and dashed lines are indistinguishable within the scale of the figure. (*a*) Results for a low density state with $y = 0.1690$, $\rho^* = 0.115\,28$. (*b*) Results for a high density state with $y = 0.3974$, $\rho^* = 0.271\,06$.

In what follows we shall use equations (36) and (37) to compute site–site correlation functions. In figure 6 the g_{33} site–site correlation function is shown at (*a*) low and (*b*) high densities. In figure 7 the g_{55} function (i.e. the correlation function between the smallest sites of the molecule) is presented for (*a*) low and (*b*) high density systems. The results in figures 6 and 7 were obtained for the racemic mixture. Figures 6 and 7 also show the site–site correlation function between R molecules (solid lines) and between an R and an S molecule (dashed line). As can be seen, in the racemic mixture site–site correlation functions between two R molecules and between an R and an S molecule are indistinguishable at both low densities and high densities. We should mention that the inclusion of exchange moves (i.e. an

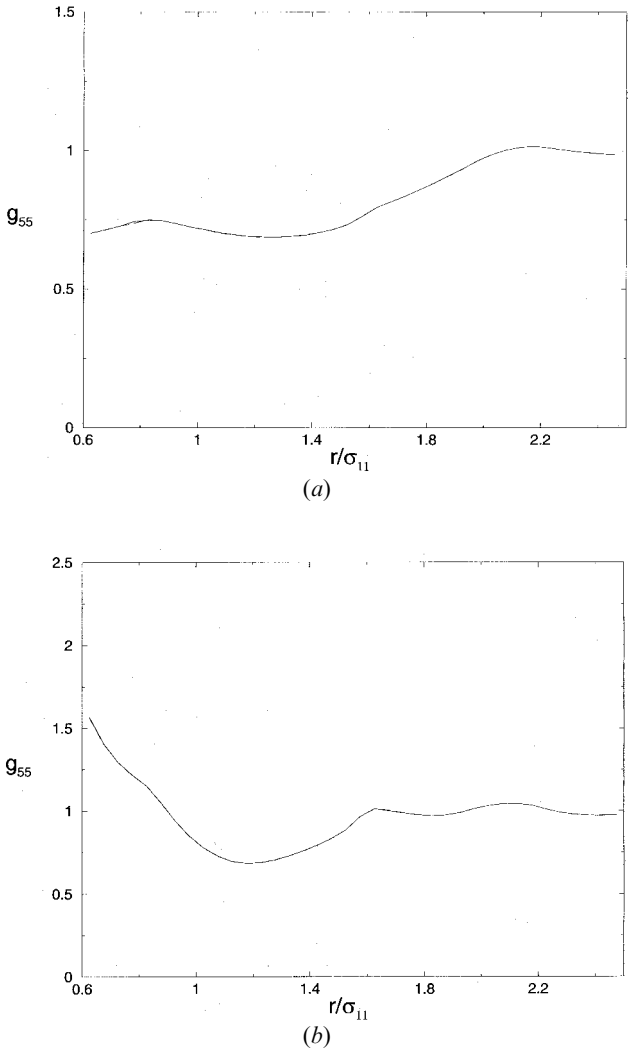

Figure 7. g_{55} in the racemic mixture obtained from the NVT simulations of this work: full line, g_{55}^{RR}; dashed line, g_{55}^{RS}. Note that the full and dashed lines are indistinguishable within the scale of the figure. (*a*) Results for a low density state with $y = 0.1690$; $\rho^* = 0.115\,28$. (*b*) Results for a high density state with $y = 0.3974$, $\rho^* = 0.271\,06$.

R and an S molecule exchanging their positions) is absolutely necessary when analysing structural differences. When the exchanges moves are not included it is possible to observe differences between RR and RS correlations (even at low densities). These differences are indicative of incomplete equilibration rather than physical differences. In fact these differences disappear completely once exchange moves are included. We do not observe differences in the racemic mixture between RR and RS correlations, and if they exist then certainly they are smaller than the accuracy of our calculations (i.e. 0.004). The striking similarity between RR and RS site–site correlation functions in the racemic mixture shown in figures 4 (*c*, *d*), 6 and 7 suggest that they may indeed be identical. Indeed, we checked all possible site–site correlation functions (i.e. $g_{12}, g_{13}, \ldots$), and again the same scenario as that shown in figures 6 and 7 appears. Although we do not have a mathematical proof, our results strongly suggest that for a racemic mixture g_{ij}^{RR} is indeed identical to g_{ij}^{RS}. In other words, at the level of site–site correlation functions, no distinction is made in a racemic mixture between RR and RS correlations. This is probably one of the most important results of this work. We searched in the literature for some evidence, or previous suggestion for this surprising finding and found that this is predicted by the RISM-HNC integral equation [22]. More simulation/theoretical work is needed in order to assess whether this surprising result is limited to the HMP studied in this work, or is a general result for any racemic mixture. Note that if g_{ij}^{RR} is identical to g_{ij}^{RS}, and since it must be equal to g_{ij}^{SS}, it means that all site–site correlation functions are identical. That may have important thermodynamic consequences concerning the possibility/impossibility of fluid–fluid phase separation in racemic mixtures.

After the surprising finding illustrated in figures 6 and 7 the natural question that arises is the following. In the racemic mixture there is no difference in site–site correlation functions between RR and RS correlations. However, does the structure of the racemic mixture differ from that of a fluid made up from molecules of a pure enantiomer, say R. In other words, are there structural differences between the racemic mixture and the pure R fluid? In figure 8, g_{11}, g_{12}, g_{13}, g_{14} and g_{15} are shown for the racemic mixture and for the pure R fluid at $y = 0.3974$. Again the results were obtained within the NVT ensemble and those presented correspond to averages of five independent runs with 400 000 cycles and $\delta r = 0.05\sigma_{11}$. Note that now we are comparing results for two different fluids, namely a pure enantiomer and the racemic mixture. This is different from the results of figures 6 and 7, where we presented RR and RS correlations in the same racemic mixture. In figure 8 the g_{11}, g_{12}, g_{13}, g_{14} and g_{15} correlation functions of the pure R fluid are close to those of the racemic mixture. However, clear differences are now visible between the pure R enantiomer and the racemic mixture, differences four to five times larger than our statistical uncertainty in g. Therefore, the differences presented in figure 8 do exist. We conclude that structural differences exist between a pure R enantiomer and a racemic mixture when the two are compared at the same number density. Larger differences between the racemic mixture and the pure R fluid were obtained for correlations involving the central atom labelled 1. These results make sense. We observe differences between the EOS of a pure R fluid and of the racemic mixture at high pressures. These differences in the EOS

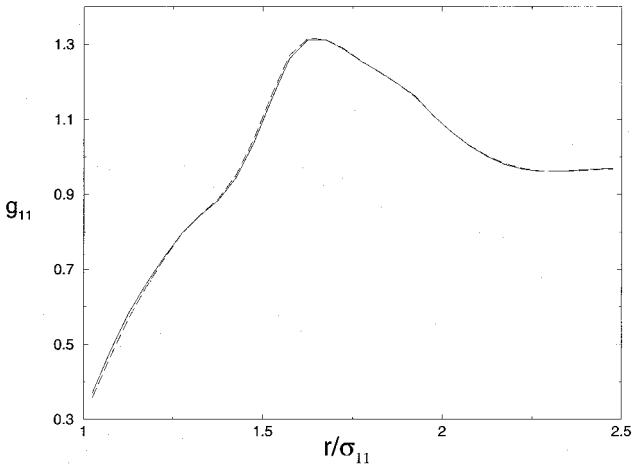

(a)

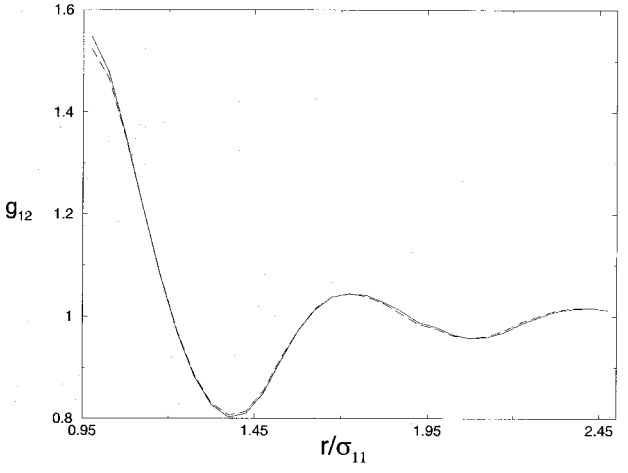

(b)

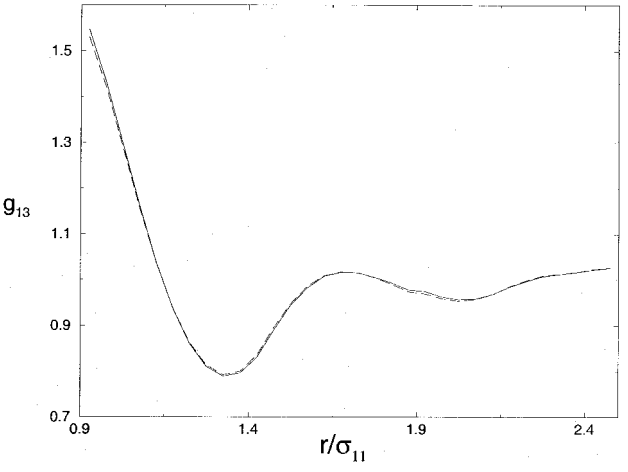

(c)

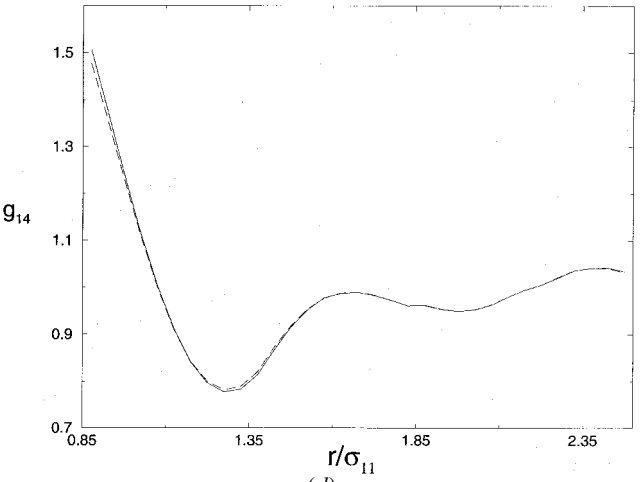

(d)

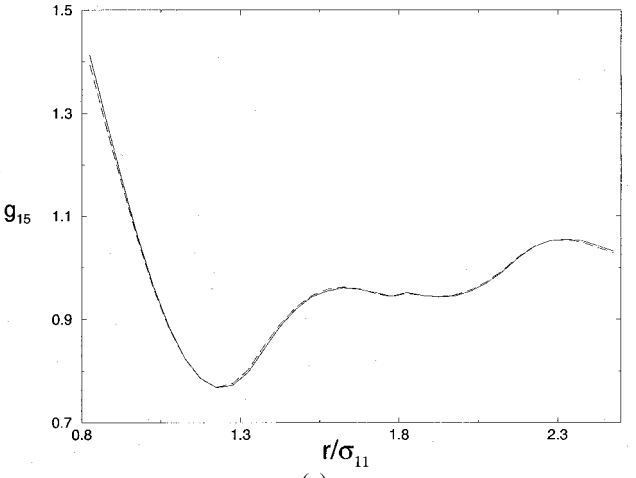

(e)

Figure 8. Site–site correlation in the pure R enantiomer (full line) and in the racemic mixture (dashed line) obtained from NVT simulations with $y = 0.3974$: with the results for (*a*) g_{11}; (*b*) g_{12}; (*c*) g_{13}; (*d*) g_{14}; and (*e*) g_{15}.

should be reflected in the structural properties. In fact for a certain density the pressure of the pure R isomer seems to be slightly higher than that of the racemic mixture. This is in agreement with the results of figure 8, where contact values for g_{1j} of the pure R enantiomer seem to be slightly higher than those of the racemic mixture.

At this point the picture emerging from our results is that a racemic mixture behaves as an almost ideal mixture. Differences found between the pure R isomer and the racemic mixture for the EOS and for the structural properties are quite small. The only differences are found at high densities, where certain indications of better packing of molecules of type R with molecules of type S (compared with RR packing) are obtained. Evidence of this is obtained from the NpT runs from the higher density of the racemic mixture with respect to the pure enantiomer, and in the NVT runs by the higher contact values of the site–site correlation functions of the pure enantiomer with respect to that of the racemic

Table 8. Virial coefficients of the HMP model as determined numerically in this work. Resutls are given in reduced units so that B_i is given in units of $V_m^{(i-1)}$. The results presented correspond to the average of four independence calculations.

B_2^{RR}	12.103 ± 0.004
B_2^{RS}	12.104 ± 0.002
B_3^{RRR}	81.06 ± 0.05
B_3^{RRS}	81.07 ± 0.03
B_4^{RRRR}	308.4 ± 0.2
B_4^{RRRS}	308.4 ± 0.2
B_4^{RRSS}	308.4 ± 0.2

mixture (when both are compared at the same number density). We must again stress that differences are quite small.

In order to analyse the low density behaviour of the EOS we have computed the second, third and fourth virial coefficients of the HPM. We evaluated these virial coefficients with high accuracy so that they are particularly appropriate for analysing differences. The results are presented in table 8. Again B_2^{RR} and B_2^{RS} are identical to within statistical uncertainty. The same occurs for B_3^{RRR} and B_3^{RRS} and for B_4^{RRRR} and B_4^{RRRS} and B_4^{RRSS}. Taking into account the accuracy of our calculations, we can say that the differences between B_2^{RR} and B_2^{RS} (if any) are smaller than 1/3000, between B_3^{RRR} and B_3^{RRS} (if any) are smaller than 1/1600 and between B_4^{RRRR}, B_4^{RRRS}, B_4^{RRSS} (if any) are smaller than 1/1540. Of course an open question is whether differences may be larger for higher virial coefficients (i.e. fifth, sixth, ...).

Our study of the HPM has not revealed big differences between the R isomer pure fluid and the racemic mixture. Since experimentalists have determined excess properties of real mixtures of racemic compounds we decided to analyse in detail a mixture of molecules with attractive forces, to see if differences emerge when attractive forces are included. For that purpose the HPM has been replaced by a model with the sites located in the same position as in the HPM model, but replacing the hard sphere interaction by a Lennard-Jones interaction (and with the simple prescription $\varepsilon_{ii} = \sigma_{ii}$) as described in § 2.

3.2. *Results for the Lennard-Jones primitive model of a chiral molecule*

In table 9 the simulation results of this work for the LJPM are presented for the pure R isomer and for the racemic mixture at a supercritical isotherm (i.e. $T^* = T/(\varepsilon_{11}/k) = 4$. Details of the simulations were as those described above. It is seen that we do not observe

Table 9. *NpT* simulation results for the LJPM model of this work. Results are presented for the pure R isomer ρ_R^* and for the racemic mixture ρ_{RS}^*. The reduced pressure is given in units of $p^* = p/(kT/\sigma_{11}^3)$.

p^*	ρ_{RS}^*	ρ_R^*	$(U/N\varepsilon_{11})_{RS}$	$(U/N\varepsilon_{11})_R$
0.125	0.090 55	0.090 37	−3.993 85	−3.987 20
0.250	0.131 70	0.131 74	−6.041 98	−6.045 00
0.375	0.156 95	0.156 49	−7.374 10	−7.345 01
0.500	0.173 78	0.174 10	−8.282 74	−8.302 57
0.750	0.198 86	0.198 56	−9.650 14	−9.631 35
1.000	0.216 36	0.216 40	−10.583 29	−10.578 85
1.250	0.230 24	0.230 28	−11.284 82	−11.290 37
1.500	0.241 97	0.241 95	−11.859 79	−11.863 21
1.750	0.251 65	0.251 80	−12.294 58	−12.306 07
2.000	0.260 45	0.260 32	−12.679 28	−12.683 59
2.250	0.268 07	0.267 93	−12.984 30	−12.967 22
2.500	0.275 05	0.275 05	−13.241 52	−13.241 51
2.750	0.281 55	0.281 37	−13.459 12	−13.440 92
3.000	0.287 48	0.287 24	−13.645 55	−13.618 80
3.250	0.292 75	0.293 06	−13.780 33	−13.813 35

any systematic deviations in density between the pure R fluid and the racemic mixture. Sometimes the R fluid presents a higher density and sometimes a lower density than the racemic mixture. No systematic trend is found in the differences. This indicates that any differences in density shown in table 9 between the two systems are erratic, and therefore fall within the statistical error of our simulations. It is seen that for a certain pressure the system with higher density tends to have a higher internal energy. Therefore the internal energy is correlated with the average density, and no definitive conclusion can be drawn on systematic differences between the two systems. Therefore again our results, show that differences between the pure R fluid and the racemic mixture fall within the statistical uncertainty of our simulations. The same type of result as for the HPM model are obtained here.

In figure 9 a comparison is shown between the implementation of Wertheim's theory proposed in this work and the simulation results (*a*) for the EOS and (*b*) for the internal energy. As can be seen, the agreement is excellent for the EOS and fair for the internal energy.

Figure 10 presents the g_{15} and g_{55} site–site correlation functions as obtained from *NVT* simulations ($T^* = 4$ and $\rho^* = 0.2419$) of the LJPM model for the pure R fluid and for the racemic mixture. The results presented correspond to the average of three independent runs (300 000 cycles were used for determining average properties in each run). The width of the grid used to determine the site–site correlation functions was $\delta r = 0.05\sigma_{11}$. Again no difference was found between g_{15}^{RR} and g_{15}^{RS} in the racemic mixture. The same is true

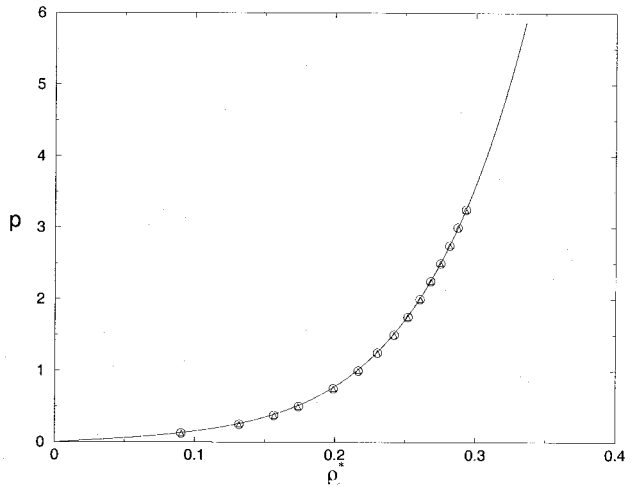

(*a*)

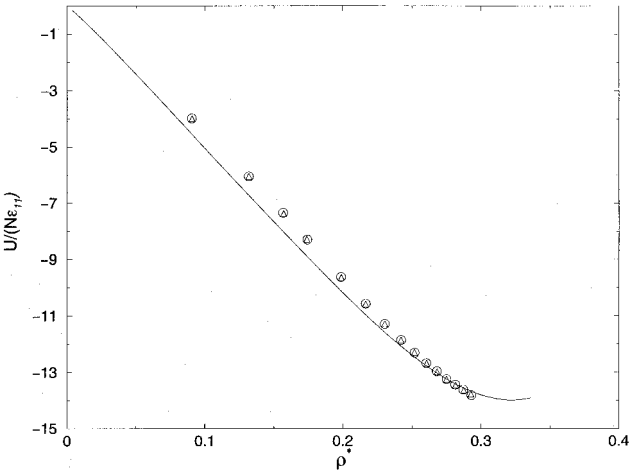

(*b*)

Figure 9. Results for the LJ primitive model proposed in this work for $T^* = 4$ obtained from the theory of this work (lines) and from simulation for the pure R enantiomer (open circles) and for the racemic mixture (open triangles): (*a*) results for the EOS; and (*b*) results for the residual internal energy.

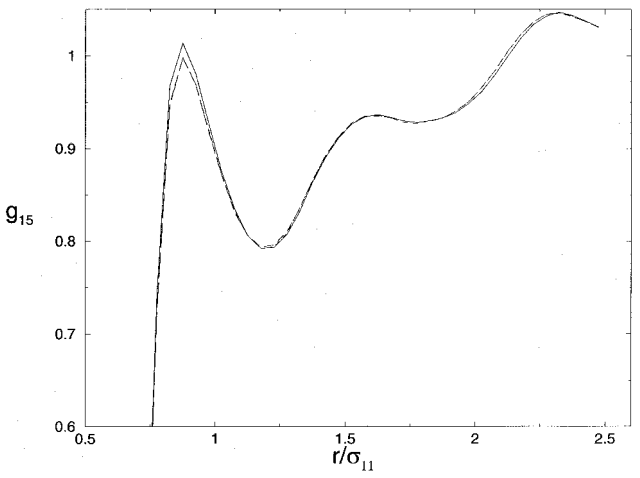

(*a*)

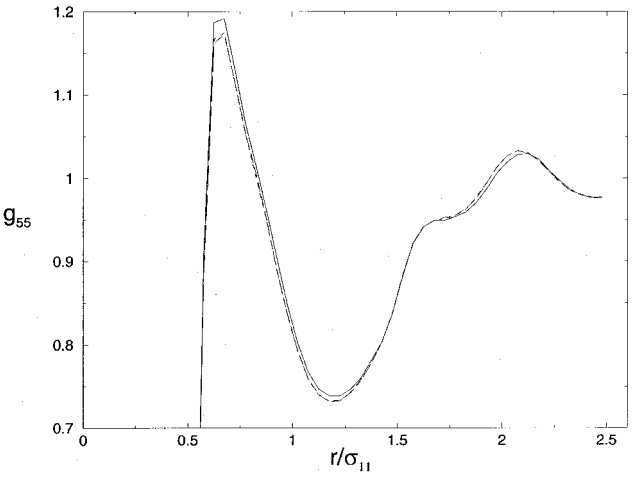

(*b*)

Figure 10. Site–site correlation functions for the LJPM at $T^* = 4$ and $\rho^* = 0.2419$ obtained from NVT simulations: full line, results for the pure R fluid; long dashed line, RR correlations in the racemic mixture; and short dashed lines, RS correlations in the racemic mixture. Note that the long and short dashed lines are indistinguishable at the scale of the figure. (*a*) g_{15} correlation function, and (*b*) g_{55} correlation function.

for g_{55}^{RR} and g_5^{RS} in the racemic mixture. That gives further support to our suggestion that RR and RS site–site correlation functions are identical in a racemic mixture. In figure 10 the site–site correlation functions for the pure R enantiomer are also presented. Clear structural differences between the pure R enantiomer and the racemic mixture are visible. Thus the results for the LJPM support all our previous findings for the hard system.

4. Conclusion

All experimental studies on racemic mixtures have found very small excess properties: these types of mixture are quite close to ideal in their behaviour. Excess volumes for these kinds of mixture are of about 0.01% of the molar volume of the system [17], and excess enthalpies are of similar magnitude. In view of that it is not surprising that the main finding of this work is the strong similarity found between the pure enantiomeric fluid and the racemic mixture, for both the hard model and the Lennard-Jones model. In fact only at high densities do we observe some small differences between the two systems, both in the equation of state and in the structural properties. The differences found are much larger than our statistical uncertainties, so that we are

confident about the fact that these differences do indeed exist. Differences found are consistent with better packing between different pair of molecules (R with S) with respect to the packing between identical pairs of molecules (R with R). Better packing between unlike molecules may be the reason why racemate compounds are often found in the solid phase of racemic mixtures. In fact, the formation of a compound R:S (1:1) may yield higher close packing density than the pure R and S in the solid phase, and the formation of racemate compounds is found in 90% of the cases for racemic mixtures, versus the formation of conglomerates (i.e. R and S crystallizing into different crystals), which appears in only 10% of the cases (Pasteur's classic example of sodic tartrate belonging to this second group). The formation of solid solutions is relatively rare (i.e. less than 1%).

One general issue that appears from this study is the difficulty in obtaining excess properties of chiral mixtures from computer simulations. In fact, this is a major problem, since the magnitude of the excess properties will in general be smaller than the statistical uncertainty of the simulations. It is our feeling that computer simulations may prove to be more useful in studying racemic mixtures in the solid phase, and probably it is for solid phases where computer simulations can help us understand the rich behaviour exhibited by mixtures of chiral compounds.

In this work, our goal was to choose a simple model of a racemic mixture for which a good theoretical EOS is available (namely the BHS), and to perform simulations to analyse possible differences between the pure enantiomer and the racemic mixture. The main outcome is that the differences are quite small, and fall for most of the cases (except at very high densities) within the range of the statistical error. The inclusion of attractive forces via the LJ model does not substantially change this conclusion. One interesting result of this work is that in the racemic mixture we did not find differences in site–site correlation functions between RR pairs and RS pairs. If differences exist they are smaller than the statistical uncertainty of our g_{ij} (typically 0.004). We suggest that they may indeed be identical. More work is needed to analyse this point in more detail, to see if it holds for other models, and whether it can be proved from geometrical considerations.

To the best of our knowledge no previous calculations have been performed for the virial coefficients between mixtures of optically active molecules. This gap is filled by the present work. Again, we did not find differences between the virial coefficients (up to the fourth) of the pure enantiomeric fluid and those of the racemic mixture. They agree within our statistical error.

A natural question arising from our work is whether one can obtain or derive a model for which larger differences may be found between the pure enantiomer and the racemic mixture. Then what geometrical or energetical factors will enhance the differences between pure fluids and racemic mixtures? Can our HPM model (or its LJ counterpart) version be modified to observe large differences? At this point we do not know the answers to these interesting questions. We feel that the search of other models for which differences may be larger may be worthwhile in order to understand the factors that contribute to making a racemic mixture less ideal. When dealing with hard bodies, usually one introduces a non-sphericity parameter α. The larger the value of α, the more anisotropic is the molecule. Usually α can be obtained if the second virial coefficient between the hard bodies is known. It would be quite useful to introduce a chirality parameter, measuring differences between the interactions between pairs of identical molecules and pairs of specular molecules. One possibility for this parameter would be

$$\chi = \frac{B_2^{\mathrm{RS}} - B_2^{\mathrm{RR}}}{B_2^{\mathrm{RR}}}, \tag{38}$$

which will measure differences between like and unlike interactions between pairs of molecules at the level of the second virial coefficient. A value of zero would be indicative of a quasi-ideal mixture, whereas a high value of χ would be indicative of a mixture that probably will exhibit important differences from ideality. In this work, the value of χ (for the hard HPM) is zero (at least within the statistical uncertainty of our calculations). Is there any geometrical factor that could make the value of χ larger, or is the zero (or almost zero) value of χ a general feature of nature? Certainly further work on this issue is needed. Virial coefficient calculations can be a useful tool for obtaining relevant information since they are performed with considerably less computational effort, and can yield higher accuracy than other numerical techniques, for instance, Monte Carlo simulations.

In a sense this work is just a first step towards the study of a problem that has received very little attention from either the experimental or the theoretical community.

Financial support has been provided by project No. BFM2001-1420-C02-01 of the Spanish DGES (Dirección General de Enseñanza Superior). J.L. would like to thank the Ministerio of Education for a 3 months travel grant to visit Complutense University. We also thank Dr Carl McBride for his help in preparing figure 1.

References

[1] Gray, C. G., and Gubbins, K. E., 1984, *Theory of Molecular Fluids* (Oxford University Press).
[2] Shing, K. S., and Gubbins, K. E., 1982, *Molec. Phys.*, **45,** 129.
[3] Wojcik, M., and Gubbins, K. E., 1984, *Molec. Phys.*, **51,** 951.
[4] Vega, C., and Gubbins, K. E., 1992, *Molec. Phys.*, **75,** 881.
[5] Chapman, W. G., Jackson, G., and Gubbins, K. E., 1988, *Molec. Phys.*, **65,** 1.
[6] Chapman, W. G., Jackson, G., and Gubbins, K. E., 1988, *Molec. Phys.*, **65,** 1057.
[7] Walsh, J. M., and Gubbins, K. E., 1990, *J. phys. Chem.*, **94,** 5115.
[8] Boublik, T., Vega, C., and Pena, M. D., 1990, *J. chem. Phys.*, **93,** 730.
[9] Johnson, J. K., Muller, E. A., and Gubbins, K. E., 1994, *J. phys. Chem.*, **98,** 6413.
[10] Cotton, F. A., 1971, *Chemical Applications of Group Theory* (New York: Wiley).
[11] Morrison, R. T., and Boyd, R. N., 1987, *Organic Chemistry* (Boston: Allyn and Bacon).
[12] Lehninger, A. L., 1982, *Principles of Biochemistry* (New York: Worth).
[13] Atik, Z., Ewing, M. B., and McGlashan, M. L., 1983, *J. chem. Thermodynam.*, **15,** 159.
[14] Atik, Z., Ewing, M. B., and McGlashan, M. L., 1981, *J. phys. Chem.*, **85,** 3300.
[15] Guette, J. P., Boucherot, D., and Horeau, A., 1973, *Tetrahedron Lett.*, **6,** 465.
[16] Stinson, S. C., 2000, *Chem. Eng. News*, 23 October, 55.
[17] Lepori, L., and Koppenhoeffer, B., 1994, *J. phys. Chem.*, **98,** 6862.
[18] Jacques, J., Collet, A., and Wilen, S. H., 1981, *Enantiomers, Racemates and Resolution* (New York: Wiley).
[19] Eliel, E. L., and Wilen, S. H., 1994, *Stereochemistry of Organic Compounds* (New York: Wiley).
[20] Pasteur, L., 1848, *C.R. Acad. Sci. Paris*, **26,** 535.
[21] Kenney, J. F., and Deiters, U. K., 2000, *Phys. Chem. chem. Phys.*, **2,** 3163.
[22] Vatamanu, J., and Cann, N. M., 2001, *J. chem. Phys.*, **114,** 7993.
[23] Vlot, M. J., Claassen, S., Huitema, E. A., and van der Eerden, J. P., 1997, *Molec. Phys.*, **91,** 19.
[24] Sholl, D. S., Asthagiri, A., and Power, T. D., 2001, *J. phys. Chem.*, **105,** 4771.
[25] Barker, J. A., and Henderson, D., 1976, *Rev. mod. Phys.*, **48,** 587.
[26] Weeks, J. D., Chandler, D., and Andersen, H. C., 1971, *J. chem. Phys.*, **54,** 5237.
[27] Boublik, T., and Nezbeda, I., 1986, *Collect. Czech. chem. Commun.*, **51,** 2301.
[28] Fan, Y., Finn, J. E., and Monson, P. A., 1993, *J. chem. Phys.*, **99,** 8238.
[29] de Miguel, E., Martin del Rio, E., and Telo da Gama, M. M., 1995, *J. chem. Phys.*, **103,** 6188.
[30] Rowlinson, J., and Swinton, F., 1982, *Liquids and Liquid Mixtures* (London: Butterworth).
[31] Allen, M., and Tildesley, D. J., 1987, *Computer Simulation of Liquids* (Oxford: Clarendon Press).
[32] Boublik, T., and Nezbeda, I., 1980, *Czech. J. Phys.* B, **30,** 121.
[33] Nezbeda, I., Labik, S., and Malijevsky, A., 1989, *Collect. Czech. chem. Commun.*, **54,** 1137.
[34] Karaaslan, H., and Yursver, E., 1991, *Chem. Phys. Lett.*, **187,** 8.
[35] Ree, F. H., and Hoover, W. G., 1964, *J. chem. Phys.*, **40,** 939.
[36] Rigby, M., 1970, *J. chem. Phys.*, **53,** 1021.
[37] Vega, C., 2000, *Molec. Phys.*, **98,** 973.
[38] Vega, C., Labaig, J. M., MacDowell, L. G., and Sanz, E., 2000, *J. chem. Phys.*, **113,** 10398.
[39] Wertheim, M. S., 1984, *J. statist. Phys.*, **35,** 19.
[40] Wertheim, M. S., 1984, *J. statist. Phys.*, **35,** 35.
[41] Wertheim, M. S., 1986, *J. statist. Phys.*, **42,** 459.
[42] Wertheim, M. S., 1986, *J. statist. Phys.*, **42,** 477.
[43] Wertheim, M. S., 1987, *J. chem. Phys.*, **87,** 7323.
[44] Archer, A. L., and Jackson, G., 1991, *Molec. Phys.*, **73,** 881.
[45] Amos, M. D., and Jackson, G., 1991, *Molec. Phys.*, **74,** 191.
[46] Amos, M. D., and Jackson, G., 1992, *J. chem. Phys.*, **96,** 4604.
[47] Boublik, T., 1970, *J. chem. Phys.*, **53,** 471.
[48] Mansoori, G. A., Carnahan, N. F., Starling, K. E., and Leland, T. W., 1971, *J. chem. Phys.*, **54,** 1523.
[49] Blas, F. J., and Vega, L. F., 1997, *Molec. Phys.*, **92,** 135.
[50] Hansen, J. P., and McDonald, I. R., 1986, *Theory of Simple Liquids* (London: Academic Press).
[51] Johnson, J. K., and Gubbins, K. E., 1992, *Molec. Phys.*, **77,** 1033.
[52] Vega, C., and MacDowell, L. G., 2000, *Molec. Phys.*, **98,** 1295.
[53] Abascal, J. L. F., and Bresme, F., 1992, *Molec. Phys.*, **76,** 1411.
[54] Sear, R. P., Amos, M. D., and Jackson, G., 1993, *Molec. Phys.*, **80,** 777.